Broadband light generation by noncollinear parametric downconversion

Silvia Carrasco, Magued B. Nasr, Alexander V. Sergienko, Bahaa E. A. Saleh, and Malvin C. Teich

Department of Electrical and Computer Engineering and Department of Physics, Boston University, 8 Saint Mary's Street, Boston, Massachusetts 02215

Juan P. Torres and Lluis Torner

ICFO-Institut de Ciències Fotòniques, and Department of Signal Theory and Communications, Universitat Politecnica de Catalunya, 08034 Barcelona, Spain

Received August 19, 2005; accepted September 25, 2005

Broadband light generation is demonstrated by noncollinear spontaneous parametric downconversion with a cw pump laser. By use of a suitable noncollinear phase-matching geometry and a tightly focused pump beam, downconverted signals that feature a bell-shaped spectral distribution with a bandwidth approaching 200 nm are obtained. As an application of the generated broadband light, submicrometer axial resolution in an optical coherence tomography scheme is demonstrated; a free-space resolution down to 0.8 μm was achieved. © 2006 Optical Society of America

OCIS codes: 190.2620, 190.4410.

Broadband optical sources are needed for many current scientific and technological applications as diverse as wavelength division multiplexing, signal generation and amplification for telecommunications,[1] generation of short pulses[2] and phase-stabilized pulses,[3] optical metrology,[4] tunable high-precision spectroscopy,[5] and optical coherence tomography (OCT).[6] A powerful route to generating broadband light is supercontinuum generation. Currently, pulsed solid-state lasers in combination with photonic-crystal fibers and tapered fibers[7] make supercontinuum generation a promising technique that is being exploited to produce broadband spectral sources. However, for most applications, a smooth rectangular or quasi-Gaussian spectrum, together with a high bandwidth, is desirable. A salient example of this need is OCT, a noninvasive imaging technique with many applications in biology and medicine, in which axial resolution is thus enhanced by the use of a broadband source.[8,9] However, irregular spectral profiles cause sidelobes to appear in the acquisition interferograms[10] and thereby adversely affect the quality and precision of the measurements.

The spectrum obtained by use of photonic-crystal fibers is often nonuniform and can even contain gaps, which limit their usefulness. The supercontinuum light generated by such sources can be optimized by either of two approaches. One is the use of spectral shapers to smooth the envelope (see, for example, Ref. 11). However, these filters must be designed for a specific operating wavelength, and their performance is restricted as a result of their limited spectral range and high losses. The second approach relies on optimizing the conditions under which the supercontinuum is generated, including using input pulses with different chirps, polarizations, and powers as well as fibers with different lengths and core sizes.[12] However, by and large, the generation of smooth bell-shaped spectra is complicated and cumbersome.

A potential alternative for specific applications is parametric downconversion. Quadratic nonlinearities have been considered for broadband tunable generation in most of the applications mentioned above, as nonlinear optical-frequency conversion can be used to extend the useful wavelength range of available laser sources. For example, important advances have been made by use of ultrashort-pulse nonlinear frequency conversion in aperiodic quasi-phase-matched lithium niobate ($LiNbO_3$).[13] However, the potential for broadband light generation based on quadratic nonlinearities in noncollinear phase-matching geometries has not yet been fully explored.

Here we demonstrate a new way to obtain broadband light based on noncollinear spontaneous parametric downconversion. With reasonable pump intensities, the source generates a low power output, a property that restricts its potential applications. However, it is robust, easy to implement, and, importantly, offers the possibility of readily engineered spectra with greatly enhanced bandwidths. In principle, such sources can be made to operate at many different central frequencies that may be of interest, including those for which other broadband sources are not available. Indeed, noncollinear parametric downconversion in a quasi-phase-matched crystal has been shown to be a source of broadband infrared light.[14] Moreover, it was shown theoretically that there is a direct relation between the spatial shape of the pump laser beam and the spectral properties of the downconverted light in such geometries.[15]

The central point of our scheme is the use of an appropriate noncollinear angle, together with a tightly focused pump beam, a recipe that makes possible the generation of downconverted photons with clean broadband spectral shapes. To illustrate the application of the technique, we demonstrate submicrometer axial resolution in an OCT configuration.

The experimental setup is sketched in Fig. 1. Light from a monochromatic cw Kr^+-ion laser, operated at a wavelength $\lambda_p = 406$ nm, after passing through a prism and an aperture (not shown) to remove the spontaneous glow of the laser tube, pumps a 1.5 mm

0146-9592/06/020253-3/$15.00

long type I lithium iodate ($LiIO_3$) nonlinear crystal, cut at $\theta = 41.7°$ for degenerate collinear phase matching. Proper rotation of the nonlinear crystal permits phase matching at the desired noncollinear angle. Lenses of different focal lengths are placed before the crystal to control the input pump beam waist. The downconversion angle selected for our purposes was $\phi = 9°$. The formalism of Ref. 15 for the single-photon-detection case predicts a clean, broad, bell-shaped spectrum for tightly focused pump beams, with beam waists of the order of 1 μm for this angle, a prediction confirmed by our observations.

The signal beam, of central wavelength $\lambda_0 = 812$ nm, is directed into a Michelson interferometer (labeled MI in Fig. 1). After passing though a variable-sized aperture and a long-pass filter with cutoff wavelength 515 nm, removing the residual pump radiation, the output of the MI is focused into a multimode optical fiber and directed to a single-photon-counting detector (EG&G, SPCM-AQR-15). By moving the mirror in steps of 30 nm in the reference arm (M) of the MI, we were able to obtain the OCT interferogram of the sample (S) placed in the other arm. All optical components of the system were selected to provide optimal performance in the 400–1000 nm wavelength range. The typical power at the detector for our system was of the order of picowatts. However, notice that optimized spontaneous parametric downconversion sources, employing periodically poled materials with large effective nonlinearities and pumped with higher-power lasers, can produce output powers of the order of several microwatts.[16]

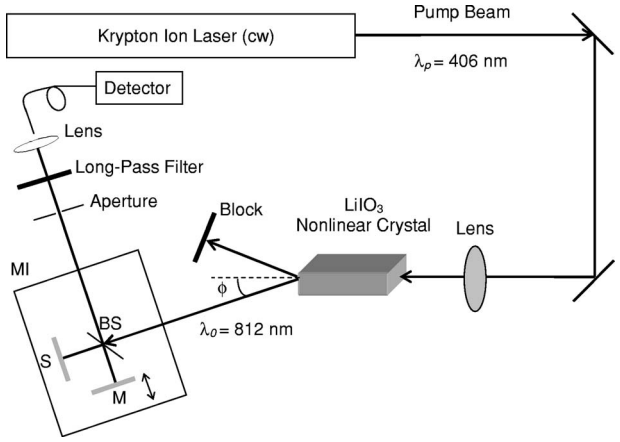

Fig. 1. Experimental setup. BS, beam splitter.

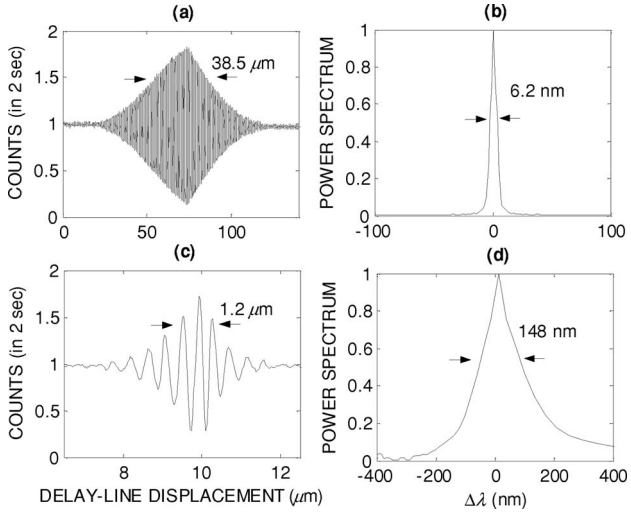

Fig. 2. (a), (c) Measured interference fringes normalized to the constant-background value versus the displacement of the delay line. (b), (d) Normalized power spectrum (obtained from the Fourier transform of the envelope of the interferogram) for a reflective mirror sample and two spot sizes of the input pump beam. (a), (b) 131 μm spot size pump beam. (c), (d) 2.6 μm spot size pump beam. The downconversion angle was $\phi = 9°$, the total pump power was 50 mW, and a 1 mm detection aperture with a 2 s counting time was used.

The spectral width, hence the attainable resolution in the OCT scheme, was predicted to depend on the pump beam waist,[15] potentially opening the possibility of tailoring the spectral bandwidth of a given crystal by proper selection of the pump-beam width. Our experimental data confirm such expectations, as illustrated in Fig. 2, where we display the drastic difference encountered for two different input pump-beam waists. In Figs. 2(a) and 2(c) we plot the observed interference patterns for a sample that comprises a mirror, normalized to the constant background. In Figs. 2(b) and 2(d) we plot the corresponding power spectra versus deviation of the wavelength from its central value, $\Delta\lambda = \lambda_s - \lambda_0$. The power spectrum of the source is obtained by Fourier transforming the envelope of the interferogram.[17] For a large pump beam of 131 μm (upper row) a resolution of 38.5 μm and a power spectrum with a FWHM value of 6.2 nm were obtained. However, resolutions of 1.2 μm and a power spectrum of 148 nm FWHM were obtained when the pump was focused down to beam waists of $\sim$2.6 μm (bottom row). Visibilities of 85% were obtained. The results are in excellent agreement with the predictions presented in Ref. 15.

Notice that spectra broader than the one presented here should be achievable in this configuration by focusing the input pump beam more tightly. Input pump-beam waists of $\sim$1 μm provide a resolution of 0.8 μm in air for $\phi = 9°$ and a clean spectrum with a width of 185 nm. The measured spectral width in this case is smaller than the theoretical calculation, mainly because of the limited spectral response of the silicon avalanche photodiode single-photon-counting detector. The measured interferogram and its envelope are displayed in Figs. 3(a) and 3(b), respectively, for this case. The visibility attained was 42%. However, enlarged visibilities can be obtained for smaller detection apertures. Visibilities of 85% were obtained by use of a detection aperture of 1 mm. The scans were taken in a few minutes. Although speed optimization is beyond the scope of this Letter, notice that Fourier domain schemes can be used to drastically increase the speed of the measurement.

As a further confirmation, we used the generated broadband light to image the thickness of a thin film. For that purpose, we replaced the reflective mirror with a sample that comprised a polymer-film membrane of refractive index $n = 1.47$ and thickness $L = 1.6$ μm. The OCT interferogram is expected to con-

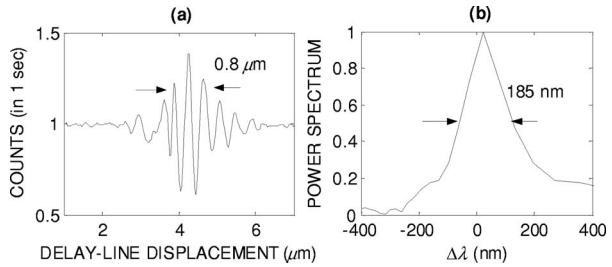

Fig. 3. (a) Measured interference fringes normalized to the constant-background value versus the displacement of the delay line. (b) Normalized power spectrum (obtained from the Fourier transform of the envelope of the interferogram) for a 1 μm spot size pump beam of 30 mW total power. The downconversion angle was $\phi=9°$, and a 1 s counting time with the detection aperture fully open was used.

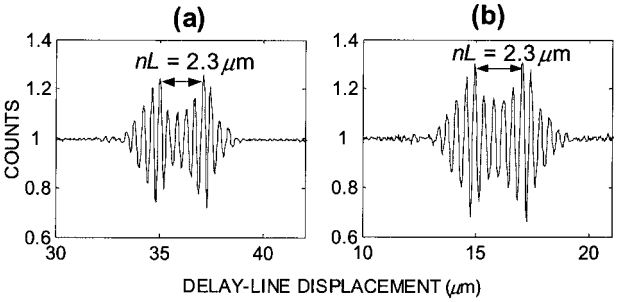

Fig. 4. Normalized interferograms for a 1.6 μm thick polymer-film membrane of refractive index 1.47 for two detection apertures: (a) a fully opened detection aperture with a 1 s counting time and (b) a 1 mm detection aperture with a 2 s counting time. The downconversion angle was $\phi=9°$, and the pump beam, of total power 30 mW, was focused to a 1 μm spot.

sist of a double-peaked envelope corresponding to the two surfaces of the sample, each with a visibility calculated to be 36%, and with their centers separated by the optical path length of the sample, $nL=2.3$ μm. The experimental result is displayed in Fig. 4(a). The peaks of the envelope, separated by $nL=2.3$ μm, exhibit a visibility of 27%. Enhanced visibilities can be obtained by use of smaller detection apertures, as illustrated in Fig. 4(b), for which the same interferogram was collected with the detection aperture reduced to 1 mm. The 32% visibility obtained in this case is very close to the theoretical value, although larger exposition times are required in this case.

To conclude, it is worth noting that spectral bandwidths higher than the one obtained with the scheme demonstrated here are achievable with schemes based on photonic-crystal fibers pumped with pulsed lasers. For example, with a source pumped by a Ti:sapphire laser with sub 10 fs/pulses, OCT resolutions of $\sim$0.75 μm at a central wavelength of 725 nm have been reported.[18] However, in contrast to such schemes, our source employs a cw pump laser, can be made to operate over a wide range of different central frequencies, and, importantly, produces bell-shaped spectra without the need for any spectral shapers. For the conditions of our experiment, the source operates at picowatt power levels. However, note that orders-of-magnitude improvements are achievable by making use of optimized schemes such as parametric downconversion in quasi-phase-matched periodically poled nonlinear crystals. Quasi-phase-matching engineering also permits noncollinear geometries. Finally, we stress that our results are relevant to a wide range of applications for which broadband light is required.

This research was supported by the Fulbright Program and the Spanish Ministry of Education and Science; by grant FIS2004-03556 from the government of Spain; by the Center for Subsurface Sensing and Imaging, a U.S. National Science Foundation Engineering Research Center; by a U.S. Army Research Office Multidisciplinary University Research Initiative grant; and by the David & Lucile Packard Foundation. S. Carrasco's e-mail address is carrasc@fas.harvard.edu.

References

1. H. Takara, T. Ohara, K. Mori, K. Sato, E. Yamada, Y. Inoue, T. Shibata, M. Abe, T. Morioka, and K.-I. Sato, Electron. Lett. **36**, 2089 (2000).
2. A. Baltuska, Z. Wei, M. S. Pshenichnikov, D. A. Wiersma, and R. Szipoecs, Appl. Phys. B **65**, 175 (1997).
3. A. Apolonski, A. Poppe, G. Tempea, Ch. Spielman, Th. Udem, R. Holzwarth, T. W. Haensch, and F. Krausz, Phys. Rev. Lett. **85**, 740 (2000).
4. S. T. Cundiff and J. Ye, Rev. Mod. Phys. **75**, 325 (2003).
5. S. T. Cundiff, J. Ye, and J. L. Hall, Rev. Sci. Instrum. **72**, 3749 (2001).
6. B. E. Bouma and G. J. Tearney, eds., *Handbook of Optical Coherence Tomography* (Marcel Dekker, 2002).
7. J. K. Ranka, R. S. Windeler, and A. J. Stentz, Opt. Lett. **25**, 25 (2000).
8. B. Bouma, G. J. Tearney, S. A. Boppart, M. R. Hee, M. E. Brezinski, and J. G. Fujimoto, Opt. Lett. **20**, 1486 (1995).
9. I. Hartl, X. D. Li, C. Chudoba, R. K. Ghanta, T. K. Ko, J. G. Fujimoto, J. K. Ranka, and R. S. Windeler, Opt. Lett. **26**, 608 (2001).
10. Y. Wang, Y. Zhao, J. S. Nelson, Z. Chen, and R. S. Windeler, Opt. Lett. **28**, 182 (2003).
11. P. C. Chou, H. A. Haus, and J. F. Brennan III, Opt. Lett. **25**, 524 (2000).
12. A. Apolonski, B. Povazay, A. Unterhuber, W. Drexler, W. J. Wadsworth, J. C. Knight, and P. St. J. Russell, J. Opt. Soc. Am. B **19**, 2165 (2002).
13. A. Galvanauskas, K. K. Wong, K. El Hadi, M. Hofer, M. E. Fermann, D. Harter, M. H. Chou, and M. M. Fejer, Electron. Lett. **35**, 731 (1999).
14. C. W. Hsu and C. C. Yang, Opt. Lett. **26**, 1412 (2001).
15. S. Carrasco, J. P. Torres, L. Torner, A. V. Sergienko, B. E. A. Saleh, and M. C. Teich, Phys. Rev. A **70**, 043817 (2004).
16. B. Dayan, A. Pe'er, A. A. Friesem, and Y. Silberberg, Phys. Rev. Lett. **94**, 043602 (2005).
17. Y.-H. Kim, J. Opt. Soc. Am. B **20**, 1959 (2003).
18. B. Povazay, K. Bizheve, A. Unterhuber, B. Hermann, H. Sattmann, A. F. Fercher, W. Drexler, A. Apolonski, W. J. Wadsworth, J. C. Knight, P. St. J. Russell, M. Vetterlein, and E. Scherzer, Opt. Lett. **27**, 1800 (2002).